Modified/Unmodified Nanoparticle Adsorbents of Cellulose Origin With High Adsorptive Potential for Removal of Pb(II) From Aqueous Solution

Azeh Yakubu (M. Sc.)
Department of Chemistry, Ibrahim Badamasi Babangida University,
Lapai, Niger State, Nigeria
Gabriel Ademola Olatunji (Ph.D-Professor)
Folahan Amoo Adekola (Ph.D-Professor)
Department of Industrial Chemistry, University of Ilorin, Ilorin, Nigeria

Abstract
          This investigation was conducted to evaluate the adsorption capacity of nanoparticles of cellulose origin. Nanoparticles were synthesized by acid hydrolysis of microcrystalline cellulose/cellulose acetate using 64% H_3PO_4 and characterized using FTIR, XRD, TGA-DTGA, BET and SEM analysis. Adsorption kinetics of Pb (II) ions in aqueous solution was investigated and the effect of initial concentration, pH, time, adsorbent dosage and solution temperature. The results showed that adsorption increased with increasing concentration with removal efficiencies of 60% and 92.99% for Azeh2 and Azeh10 respectively for initial lead concentration of 3 mg/g. The effects of contact time showed that adsorption maximum was attained within 24h of contact time. The maximum adsorption capacity and removal efficiency were achieved at pH6. Small dose of adsorbent had better performance. The kinetics of adsorption was best described by the pseudo-second-Order model while the adsorption mechanism was chemisorption and pore diffusion based on intra-particle diffusion model. The isotherm model was Freundlich. Though, all tested isotherm models relatively showed good correlation coefficients ranging from 0.969-1.000. The adsorption process was exothermic for Azeh-TDI, with a negative value of -12.812 X 10^3 KJ/mol. This indicates that the adsorption process for Pb by Azeh-TDI was spontaneous. Adsorption by Azeh2 was endothermic in nature.

Keywords: Cellulose-TDI, cellulose acetate, nanoparticles, lead, Adsorption

Introduction

The purity of water is of vital concern for mankind since it is directly linked with human welfare. Among the various pollutants encountered in water, toxic metals are highly important because they tend to remain what they are in the environment for long time which ultimately causes them to accumulate in various ecosystems of the environment (Jain, 2014; Yusoff et al. 2014; Xining et al. 2015). Methods such as flocculation, chemical oxidation, solvent extraction, electrolysis, precipitation, ion exchange membrane technologies, reverse osmosis and crystallization used for removal of toxic metals in order to produce effluents of better quality are often restricted because of several technical, economical and environmental constraints (Bhatnagar & Minocha, 2006; Sciban, 2008; Quintelas, 2009; Barakat, 2011; Jain, 2014; Yusoff et al. 2014; Xining et al. 2015). Further, abatement of metals in the above processes has been largely attempted using inorganic agents which have been again established for toxicity issues (Jain, 2014). Exposure to some metals, such as mercury and lead, may also cause development of autoimmunity, in which a person's immune system attacks its own cells (Bhatnagar & Minocha, 2006; Sciban, 2008; Quintelas, 2009; Barakat, 2011; Fu & Wang, 2011). Several types of diseases have been associated with lead poisoning due to its rapid distribution into the red blood cells followed by its re-distribution into other vital organs in the body causing diseases such as rheumatoid arthritis, diseases of the kidneys, circulatory system, nervous system, and damaging of the foetal brain at higher doses, which results to irreversible brain damages (Abdus-Salam & Adekola, 2005; Barakat, 2011; Olaniyi, 2011; Edokpayi et al. 2015). According to WHO (World Health Organization) standards, its maximum limit in drinking water is 0.05 mg/dm^3 but the maximum discharge limit for lead in wastewater is 0.5 mg/dm^3 (Hubicki & Kołodynska, 2012). Biosorbents are prepared from naturally abundant and/or waste biomass (Asadi, 2008; Barakat, 2011; Jain, 2014; Yusoff et al. 2014). They have been found to exhibit different adsorption capacities for heavy metals which are due to different functionalities on their surface. However, this capacity is low as compared to commercially ion exchange resins, but different chemical modifications (e.g. base, acid, heat and dyestuff treatments) result in improvements in the original surface properties of the materials for uses in technological applications (Asadi et al. 2008; Gurgel, 2009). This approach has made possible the synthesis of adsorbents with potentially lower costs as compared to commercially available ion-exchange resins (Asadi et al. 2008).

Cellulose is the most abundant polymer on earth, representing about 1.5 x 10^{12} tons of total annual biomass production (Rodionova et al. 2009; Azeh et al. 2011; Anna et al. 2012; Yanxia et al. 2013). Cellulose is a polysaccharide consisting of a linear chain of several hundreds to over ten

thousand β-(1→4)-linked D-glucose units (Atanu et al. 2006; Peng et al. 2011; Yanxia et al. 2013; Anuj et al. 2014; Jonas, 2014; Liu, 2015). It is a biodegradable and non-toxic biopolymer (Peng et al. 2011). It is widely available in nature and closely relevant to people´s daily life in the form of paper, textiles etc. The rod-like or whisker-shaped particles with dimensions, 3–20 nm wide, 50–2000 nm long) have a unique combination of characteristics: high axial stiffness (~150 GPa), high tensile strength (estimated at 7.5 GPa), low coefficient of thermal expansion (1 ppm/K), thermal stability up to ~300°C, high aspect ratio (10–100), low density (1.6 g/cm^3), lyotropic liquid crystalline behaviour, and shear thinning rheology in CNC suspensions (Filpponen, 2009; Rodionova et al. 2009; Stephen, 2010; Robert et al. 2011; Anna et al. 2012; Yanxia et al. 2013; Liu, 2015). Cellulose nanocrystals are needle shaped crystalline entities mainly extracted by acid hydrolysis from cellulose. The amorphous regions in the microfibrils, as well as those embedded between them are destroyed by acid hydrolysis, leaving the crystalline segments intact (Rodionova et al. 2009; Azeh et al. 2011; Anna et al. 2012; Liu, 2015). Nanocellulose, which offers a combination of biosorption, nano dimensions combined with its unique cellulosic nature, has tremendous potentials for new and green route to solve the current heavy metal pollution problems (Liu, 2015). High specific area of nanocellulose is expected to provide large number of active sites on the surface of biosorbent to immobilize metal ions. The surface functional groups functioning as metal-binding sites on the biomass irrespective of micro or nanoscale are considered responsible for immobilization of heavy metal ions (Liu, 2015). On the basis of the above problems caused by heavy metals, it is therefore, the objective of this work to employ modified/unmodified nanoparticles of cellulose origin due to their unique performance at nano scale dimensions for adsorption of Pb^{2+} ions in very dilute model water.

Material and Methods

All the chemicals used in the synthesis of nanocellulose and its derivatives were of analytical grade and obtained from BDH Chemicals Ltd (Poole England). They were used without any further purification and these include; Cellulose and H$_3$PO$_4$, Pb(NO$_3$)$_2$, HNO$_3$, NaOH were obtained from BDH Chemicals.

Preparation of Lead (II) Stock Solutions

Stock solutions of 1000 mg/L were prepared by dissolving appropriate amounts of Pb(II) and in distilled-deionized water. Adjustment of pH was accomplished using 0.1 M NaOH or 0.1 M HNO$_3$ to obtain test solutions with pH values ranging from 2 to 10.

Equilibrium Adsorption Experiment

The adsorption of Pb (II) ions by Azeh2 and Azeh4 was investigated by batch mode adsorption. The effect contact time for 120 min, solution pH (2-10), adsorbemt dosage (0.4 – 1.2 g), solution temperature (300 – 340 K) and initial concentration (1-10 mg/L) on the adsorption were investigated.

Adsorption of Pb (II) on Synthesized Nanomaterials
Effect of Initial Concentration

The synthsized samples (0.2 g) were weighed using an analytical balance and were contacted with 20 mL of an initial Pb (II) concentration of (1 to 10 mg/L) and eqilibrated on an orbital shaker for 240 min at 298 K. The mixture was filtered and analyzed on an Atomic Absorption Spectrophotometer (AAS) (iCE 3000 AA02134104 v1.30 model) at wavelength of 283.3 nm. Absorption capacity of Pb(II) ions were measured and calculated from the difference between the initial and final concentrations of Pb (Adebayo et al. 2014). The amonut adsorbed (mg/g) was calculated using the formula: $Q = (Ci - Cf)V/_W$

Where Q = Quantity of solute adsorbed from solution of volume, V (mL), C_i = Initial concentration before adsorption, C_f = Concentration after adsorption, V = Volume of adsorbate used in mL, W = Mass of the adsorbent in g

Effect of pH

The effect of pH was carried out by varying the pH (2-10) of the 20 mL 3 mg/L Pb(II) solution from 2-10 using 0.1 M NaOH or 0.1 M HNO_3 to monitor the pH of the metal solutions.

Effect of Adsobent Dose

This was carried out by using constant adsorbate of 20 mL 10 mg/L Pb(II) solution with adjusted pH to the optimal pH 6. Azeh2 and Azeh10 of dosage (0.4 – 1.2 g) was mixed with the metal solution in a 100 mL flask and the mixture was shaken for (120 min). The mixture was filtered and analyzed for residual Pb(II) ion in the filterate by atomic absorption spectroscopy.

Results and Discussion
## Adsorption Study of Metal Ions onto Azeh2, Azeh4 and Azeh10
Effect of Initial Ion Concentration on Adsorption Behaviours of Pb(II) Ions

The nanomaterials used for the adsorption studies were from our previous studies on synthesis and characterization (Azeh et al. 2017). The equilibrium adsorption of Pb(II) ion by Azeh2 and azeh10 sample was investigated by equilibrating 20 mL of simulated aqueous Pb(II) solution of

different concentrations ranging from (1 to 10 mg/L) with 0.2 g of the adsorbent at a pH of 6.0 at 300 K for 120 min. The results of the effect of initial concentration of Pb(II) ions are shown in (**Figure 1**). The initial metal ion concentrations on adsorption behaviours being an important factor that can influence adsorption behaviours of the adsorbent. **Figure 1** showed the adsorption capacity of the adsorbents (Azeh2 and Azeh10). It was oberved that the amount of Pb(II) ions adsorbed in mg/g increased with increasing metal ion concentration and reached a maximun at 10 mg/L. The adsorption process indicates that the synthesized nanomaterials can remove high amount of metal Pb(II) ions within the initial concentration range studied in this work. A similar result has been reported by (Yusoff et al. 2014; Farre, 2015), where they used initial metal ion concentration of 1 to 50 mg/L and found that there was no further metal uptake observed above 25 mg/L. The Azeh10 sample had better performance than Azeh2 sample. This may be attributed to the presence of acetate functional groups (-COOCH$_3$-group) coupled with the presence of high number of $–OPO_3^{3—}$as the FT-IR of the synthesized nanoparticles revealed the presence of the phosphate ester groups around 900-1003 cm^{-1} for P-O, P-O-C and P-OH which appeared as shoulder vibrations while P=O bond vibration was observed around 1203 cm^{-1} on the nanomaterial`s surface (Mautner et al. 2016; Azeh et al. 2017). The presence of these groups have been reported to show high tendency of complexing with divalent metal ions through surface complexation mechanisms. This process indicates that there were more available active sites on the adsorbent surface due to the large surface area of the nanomaterials as revealed by BET in the previous study (Azeh et al. 2017). Since, increasing metal ion concentration means increase in the number of particles in the solution and implies that, the availability of active binding sites on the adsorbent surface and the large number of Pb(II) ions in soulution led to increasing amount of the adsorbate adsorbed onto the adsorbent materials. Removal efficiency up to 60 % was achieved using Azeh2 sample and up to 92.99 % of the initial lead concentration was adsorbed by Azeh10 sample. This phenomenon is expected as there are more of the particles for adsorption in solution as the initial concentration increase. Since, the adsorbent dosage was kept constant for the initial concentration (Mehmet & Şukru, 2006; Li et al. 2007; Adegoke et al. 2014). Adsorption is also complimented by the nature of the adsorbent materials. Especially, due to surface area, micropore volume, surface charge and the size of the particles and the presence of metal scavenging oxygen atoms of the phosphate ester and hydroxyl groups on the surface of nanoparticles. The existence of Phosphonated-CNC as individual particles due to electrostatic repulsion can prevent agglomeration of the particles and thereby increase the metal ion uptake. Other reports on adsorption studies showed that there is increase in adsorption with increasing concentration of

adsorbate in solution (Li et al. 2007; Adegoke et al. 2014; Suopajarvi, 2015). Different adsorption capacities for Pb(II) ions by different forms of bioadsorbents and cellulose modified by different chemical agents have been reported (Sewwandi et al. 2012; Mudasir et al. 2015). The maximum adsorption capacity obtained for the synthesized materials in this study were higher than some of the maximum sorption capacities reported for various modified cellulose materials at room temperature (Wojnarovits et al. 2010). The presence of hydroxyl (-OH), phosphonic (-OPO_3H^{2-} and -OPO_3^{3-}), sulphonate (-SO_3^{2-}, and carbonyl (CO) groups is believed to be the metal binding sites on the cellulose nanomaterials (Shatkin & Wegner, 2014; Mudasir et al. 2015). Phosphoric acid modified agricultural wastes have been reported to posse high affinity for the removal of heavy metal ions in aqueous solution as reported by (Dada et al. 2013). The presence of these groups on the synthesized Azeh2 and Azeh10 nanomaterials was revealed by FT-IR results of analysis of the samples. Moreover, sulphonic groups on the surface of the synthesized nanocellulose are likely to have a greater degree of ionization at higher pH than other functional groups in cellulose (hydroxyl or carboxyl groups), so that the electrostatic affinity of sulphonic groups for metals may be stronger and hence, increased metal uptake (Suopajarvi, 2015). Functionalized nanocellulose has been reported to show high adsorption capacities for various metal ions than their native counterpart depending on the type of modifying reagents (Liu, 2015; Hokkanen et al. 2014). The results obtained in this study are higher than those reported on the applications of CNCs for removal of Cd^{2+} and Pb^{2+} ions (Xiaolin et al. 2012). The adsorption of Pb(II) ions by the synthesized nanomaterials is also attributed to particle size, specific surface area, pore size and their microporous nature as reported by Armand (Farre, 2015) on the adsorption studies of Pb(II) and Cd(II) ions in solution.
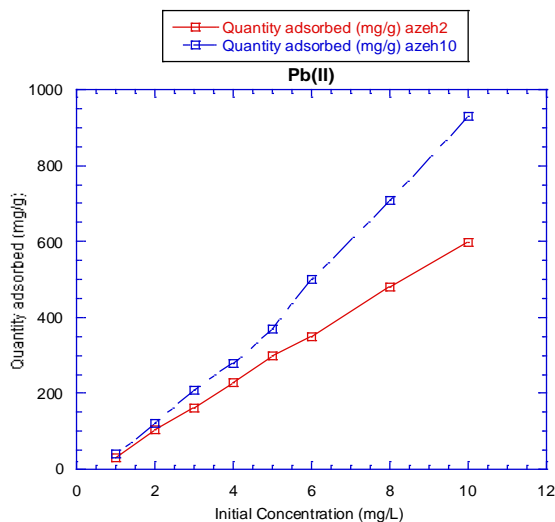
Figure 1. Effect of initial ion Concentration on the adsorption of Pb(II) ions onto Azeh2 and Azeh10 at 3 mg/L. Stirring rate: 70 rpm, time: 240 minutes: pH: 6 and temperature: 300 K, Adsorbent dose: 0.2 g

Effect of Contact Time On Adsorption of Pb(II) Ions

The effect of contact time on the adsorption of Pb(II) ions in aqueous solution is represented in **Figure 2**. The results of the adsorption rates of Pb(II) ions by Azeh2 and Azeh10 and Azeh-TDI at adsorbate concentration 3 mg/L with time at constant adsorbent dose (0.2 g) at 300 K was plotted. The results indicated that the adsorption of Pb(II) ions onto Azeh2, Azeh10 and CNC-TDI increased with increasing time and the maximum adsorption capacities achieved by the three samples; Azeh2, Azeh10 and CNC-TDI for the adsorption of Pb was 276 mg/g; 92 % removal by Azeh2; The maximum adsorption by Azeh10 sample for Pb^{2+} was 153.8 mg/g equivalence of 51.3 % removal efficiency. The TDI modified sample had 232 mg/g metal up-take and 77.33 % removal for Pb from the solution within 24 h of contact time. The three samples used had high adsorption capacities and removal efficiencies for Pb ions in solution. The rapid kinetics in this study is of immense significance for practical applications, as it facilitates the use of smaller reactor volumes which ensures high efficiency and process economy. The samples exhibited rapid increase in the absorption of Pb^{2+} up-to 6 h of contact time with the maximum amount of metals removal around 276 mg/g for Pb, while 153 mg/g amount of Pb removal was the maximum capacity achieved for Pb by Azeh2 within 24 h. Azeh-TDI modified sample had the highest amount for Pb^{2+} removal within the 6 h of contact time, while 231 mg/g removed within 24 h.

A steady increase for the removal of Pb^{2+} was observed after the attainment of the maximum metal absorption capacities by Azeh2, Azeh10

431

and Azeh-TDI samples. The formation of the adsorption plateau by the samples with a minimal increase in adsorption indicates the equilibrium of the adsorption process has been reached and limited binding sites for metal ions are now available for further up-take of Pb ions in solution. An increase in the amount of the adsorbed metal ions after the equilibrium attainment is attributed to the formation of insoluble metal hydroxides due to the pH of the metal ion solution. Fast kinetics has been documented by Armand (Farre, 2015) where the maximum equilibrium time needed for the maximum uptake of Pb, Cd and Ni was 40 min. A report by (Andal & Gohulavani, 2009) also showed that modified Indian almond nut shells adsorbed higher amounts of Cr(VI) up to 30 minutes of agitation time as no further increase in adsorption was recorded above this time. All samples indicated good adsorption performance for Pb^{2+} ions in solution and it ranged from 153.8 – 276.1 mg/g with 51.27 – 92.03 % removal efficiency. But the order of performance of the synthesized nanomaterials is Azeh2>Azeh-TDI>Azeh10 within 24 h of contact time. While the Azeh-TDI sample showed a better performance within 10 - 30 min of the agitation time with the metal solution. Generally, the high adsorption of Pb by the these samples may be due to high binding sites on the surface of the sample as a results of more number of atoms on the surface of the materials, large specific surface area of 105.7 – 250.6 m^2/g and Langmuir surface area of 10,336.2 m^2/g. Another possible reason for the high adsorption capacity of the synthesized nanomaterials for removal of Pb(II) ions in aqueous solution is due to the low concentrations of Pb(II) ions present in the solution which allows the ions to interact with two or more binding sites, effectively leading to a higher adsorption performance as reported by (Gadd, 2009; Hokkanen et al. 2012). Another possible mechanism is ion exchange with an adjacent hydroxyl group, but as with many other bioadsorbent materials, there is also a possibility that both mechanisms may be involved in the adsorption process, since there are several active groups exposed to the surface of the adsorbent being that they are nanomaterials (Gadd, 2009; Onundi et al. 2010; Hubbe et al. 2011). TDI modified sample tends to show higher adsorption and removal capacity for Pb ions in aqueous solutions than other samples not modified at lower contact time (10 – 30 min). The one explanation for this is the presence of donor atoms such as –N and O introduced on the surface of CNC nanoparticles through chemical modification of the free and accessible –OH groups probably enhanced the absorption potential of TDI modified samples.
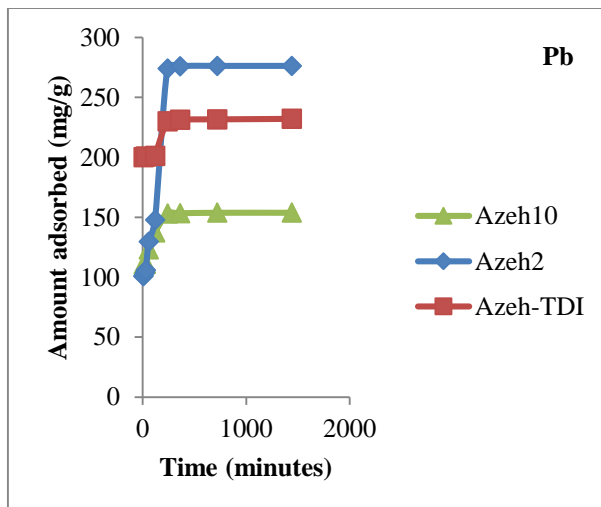
Figure 2: Effect of contact time on Adsorption of Pb (II) onto Azeh2, Azeh-TDI and Azeh10 at equilibrium concentration 3 mg/l. Stirring rate; 75 rpm, pH: 6 and Temperature 298 K
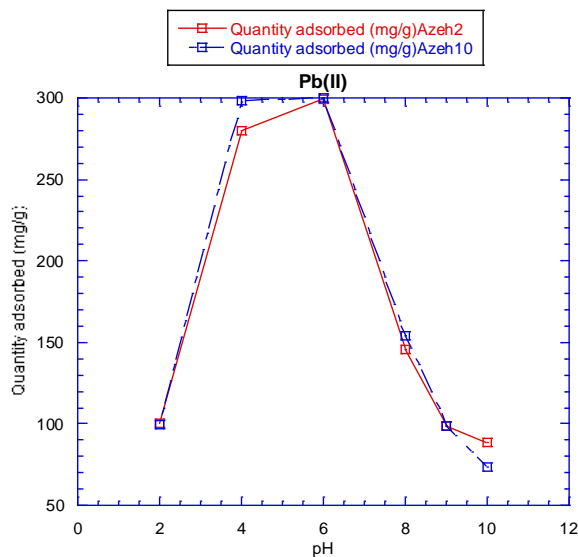
Effect of pH on Adsorption of Pb (II) Ions

The results of effect of pH on adsorption of Pb (II) ions onto Azeh2 and Azeh10 was studied over a pH range 2-10.

Effect of pH on Adsorption of Pb (II) Ions in Aqueous Solution

Solution pH is an important parameter governing the removal of metal ion from aqueous solutions (Mehmet & Şukru, 2006; Adebayo et al. 2014; Adegoke et al. 2014; Suopajarvi, 2015). It can affect the adsorbent surface charge and the degree of ionization. **Figure 3** shows the effect of pH on the adsorption behaviours. It was found that adsorption capacities of Azeh2 and Azeh10 for Pb (II) occurred over a wide range of pH 2-10 and adsorption increased with increasing pH up to pH 6. Sample Azeh2 had its maximum adsorption capacity at pH 6 with about 298.9 mg/g representing 99.63 % metal removal efficiency by the adsorbent. Sample Azeh10 showed maximum adsorption capacity at pH 6 with about 299.9 mg/g; 99.97 % Pb (II) removal. After this, the adsorption of Pb (II) by Azeh2 and Azeh10 decreased sharply due to repulsion between the positively charged surface resulting from adsorbed metal ions on the adsorbent surface and free mobile cationic species in solution and the occupation of the active binding sites on the adsorbent surface (non-availability of active sites) may also contribute to the sharp decrease in adsorption. The above reasons may also be justified by the values of the pH_{PZC} = 1.79 and 1.50 for sample Azeh2 and Azeh10. It has been reported by (Liu, 2015) that, when the pH values are lower (pH < pH_{PZC} = 1.25), the concentration of protons competing with metal ions for

the active sites is higher. Meanwhile, the adsorbent surface is positively charged and metal ions with positive charge have difficulty approaching the functional groups due to electrostatic repulsion. Thus, adsorption capacities are low at lower pH values. With the increase of pH (pH > pH_{PZC} = 1.79 and 1.50 for Azeh2 and Azeh10), the concentration of protons decreases and the adsorbent surface charge becomes negative (Suopajarvi, 2015; Thouraya et al. 2013). Therefore, the electrostatic attraction increases between the sorbate and the adsorbent, which leads to a higher adsorption capacity. Both samples showed an extended adsorption across a wide range of pH values 2-10. Since, appreciable amount of the adsorbate was removed across all the pH range 2-10. This is attributed to the fact that CNCs bear numerous hydroxyl groups and the phosphate ester groups due to treatment with phosphoric acid. In the studied pH range, the phosphate groups, which remained fully ionized, as well as the hydroxyl groups, are less affected by the pH. The optimum pH values which correspond to the maximum adsorption capacity of Pb (II) ions were observed at pH 4.0 and 6.0 for Azeh2 and Azeh10 respectively. The results agreed with the documented work by (Gurgel & Gil, 2009). An optimum pH range between pH 4.0 and 6.0 usually leaves most binding sites un-protonated and the metal binding is maximised (Gurgel & Gil, 2009). At pH 8 to 10 the increase in metal ion uptake by Azeh2 and Azeh10 was moderately slow and may be due to formation of stable hydrolysed species $Pb(OH)_2$. However, at pH 4.0 both samples showed high adsorption capacities for Pb(II) ions. Azeh10 sample had better performance at both pH 4 and 6. Afterwards, a gradual decrease in adsorption was observed from pH 8, and this trend continued to pH 10. This may be due to formation of insoluble hydroxyl complexes above the optimum pH as reported by (Gurgel & Gil, 2009; Adebayo et al. 2014; Adegoke et al. 2014). So also, the formation of $Pb(OH)_3^-$ hydrolyzed species may eventually lead to repulsion between the negatively charged adsorbent surface and thus, decrease in adsorption is inevitable. It was observed that at pH 2, the amount of metal ions removed was low, due to high number of hydrogen ions which effectively compete with Pb(II) ions for the available binding sites on the adsorbate surface. Based on this, desorption study of the synthesized cellulose nanomaterial can be achieved at pH below 2. Higher adsorption values obtained for the adsorption of Pb^{2+} ion is attributed to smaller hydrated radius of Pb^{2+} (0.401 nm), high electronegativity of Pb^{2+} and it is a hard Lewis acid than Cd^{2+} and also has high affinity for most organic functional groups including hard Lewis bases such as -COOH or -OH of phenolic compounds (Azeh et al. 2011). Generally, this study showed that the synthesized nanomaterials adsorbed appreciable amount of metal ion over a wide range of pH in the model water solution.
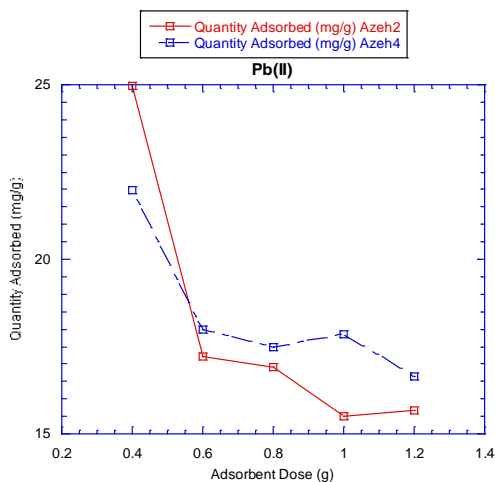
Figure 3: Effect of pH on Pb(II) ion adsorption onto Azeh2 and Azeh10 at equilibrium concentration:3 mg/L. Stirring rate: 70 rpm, time: 120 minutes: pH: 6, temperature: 300 K, adsorbent dose: 0.2 g

Effect of Adsorbent Dose on Adsorption of Pb(II) Ions

The influence of adsorbent dose on adsorption of lead at constant adsorbate concentration was studied in order to determining the appropriate mass of the nanomaterial that will bring about a better decontamination of aqueous solutions laden with Pb(II) ions. This was carried out by varying the amount of adsorbents over an adsorbent dose of 0.4 g to 1.2 g. **Figure 4** is the plot of the fractions of lead adsorbed versus adsorbent dose using Azeh2 and Azeh4 samples. The results indicated that the adsorption of Pb(II) ion by the nanomaterial is a function of the sample surface area, pore volume and size and the chemical functionalities on the surface of the adsorbents. The pore size and pore volume for the synthesized nanomaterials was 1.324 – 9.237 nm and 0.01427–0.07939 cm^3/g. Considering the size of hydrated lead(II) ions (0.410 nm) in solution it could be inferred that the adsorption of Pb(II) takes place significantly at the micropore (<1 nm) of the nanoparticles (Thouraya et al. 2013). It is observed that small amount of the materials gave maximum adsorption as reported by (Mehmet & Sukru, 2006; Liu, 2015) on synthetic hematite nanoparticles. A steady decrease in adsorption was observed with increasing amount of sample dosage which may be due to overlapping of sample active sites (Edokpayi et al. 2015). Another reason, for low amount of Pb(II) ions adsorbed with increasing adsorbent dose may be due to particle agglomeration/clustering which can lead to blockage of the active sites on the synthesized nanomaterial resulting in the reduction of the surface area, pore diameter and pore volume of the synthesized

435

nanoparticles. The maximum capacity and removal efficiency of the adsorbents Azeh2 and Azeh4 were 24.97 mg/g; 33.29 % and 21.97 mg/g; 31.31 % respectively.


Figure 4: Effect of adsorption dose on Pb (II) ion onto azeh2 and azeh4 at equilibrium concentration: Stirring rate: 70 rpm, time: 120 minutes: pH: x, Temperature: 300 K, Adsorbent dose: 0.2 to 1.2 g
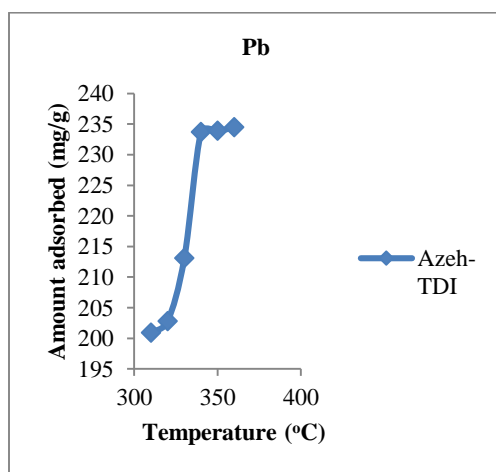
The Effect of Solution Temperature on Adsorption of Pb (II) Ion

The results of the effects of solution temperature on the adsorption of Pb (II) ions in solution was investigated by subjecting Azeh2 (Phosphonated-cellulose nanoparticle) and Azeh10 (Phosphonated-cellulose acetate nanoparticle) at 300-350 K (**Figure 5**). It was observed that the synthesized nanomaterials could perform well across the temperature range studied in this work. The results also indicated that in the temperature range studied, both samples showed high adsorption capacities up to 300 mg/g and removal efficiency of 100 %. This was an indication that the studied samples could not be affected by a 10 ºC rise in temperature of the system. Adsorption process was not affected by temperature as no further increase in adsorption or removal efficiency was observed for the samples. It was observed that the experiments conducted over the solution temperature range used showed that the adsorption of Pb(II) ions in aqueous solution was practically total (100 %). The high adsorption capacity obtained in this work is similar to the report by (Khezami et al. 2012) where he reported that microporous materials have shown higher adsorption capacities because of their large surface area compared to macroporous whose surface area is smaller. Thus, the uptake of Cu(II) and Pb(II) ions was low for macroporous activated carbon when compared with microporous carbon biosorbent. This reason is supported by the properties exhibited by the synthesized nanoparticles as their surface area, porosity and pore volume indicated that they are

microporous nanoparticles. The adsorption capacity for TDI modified sample showed that metal removal was a function of temperature as removal capacity increased with increasing solution temperature of the metal ions. The maximum metal up-take was attained for Pb at 340 K, with Pb(II) up-take of 233.7 mg/g and 78 % removal efficiency. After this maximum attainment, steadiness in the adsorption process of Pb^{2+} was observed from 450-360 K. The reason for this could best be explained by the increase in kinetic energy of the system, resulting in high mobility and frequency of contacts between reacting particles and the walls of the container, thereby, leading to high metal up-take. Thermodynamic data revealed the nature of the adsorption process to be exothermic and thermodynamically feasible.
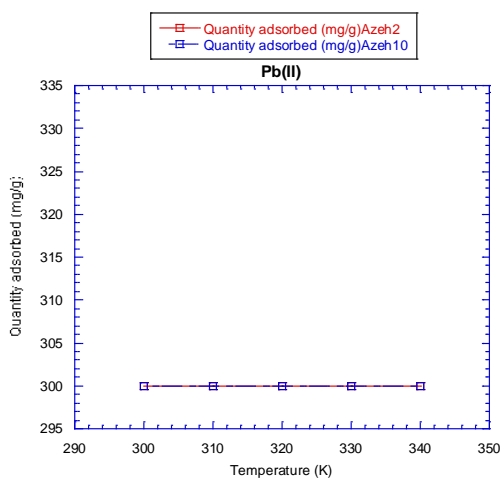
Figure 5: Effect of temperature on adsorption of Pb(II) onto Azeh2 and Azeh10 at equilibrium concentration: 20 mg/L. Stirring rate: 70 rpm, time: 120 minutes, pH: 6.0 and adsorbent dose: 0.2 g

Figure 6: Effect of temperature on Adsorption of Pb (II) onto Azeh-TDI at equilibrium concentration 3 mg/l. Stirring rate: 75 rpm, pH: 6; Adsorbate dose: 0.2g

Adsorption Isotherms

The data Pb(II) ions sorption onto three synthesized nanomaterials (Azeh2, Azeh10 and Azeh-TDI) were fitted with Langmuir, Freundlich, Temkin and D-R isotherm models in order to determine which best fits the adsorption process Pb(II) ions in aqueous solution.

Langmuir Isotherm, Freundlich, Temkin and Dubinin–Radushkevish (D-R) Figures 7-18

Parameters for Langmuir given **as** $\frac{Ce}{qe} + \frac{1}{bQm} + \frac{Ce}{Qm}$ **linearize form equ. 1** (Mohammad, 2015).

Where q_e (mg/g) is the equilibrium adsorption capacity and qm (mg/g) is the maximum amount of the ions adsorbed per unit weight of the adsorbent. The latter also describes a formation of the complete monolayer coverage on the surface at a high equilibrium H_2S concentration Ce (mg/L) and practical limiting adsorption capacity. b (L/mmol) is the Langmuir equilibrium constant related to the affinity of the binding sites and also indicates the binding energy of the adsorption reaction between adsorbate molecule and adsorbent.

Freundlich equation is given as $\mathbf{q_e = K_f\ C_e\ ^{1/n}}$ **equ. 2a**

Linearized form of the equation is logqe = logk_f + 1/n logCe equ. 2b

If the concentration of the solute in the solution at equilibrium, C_e, is raised to the power of $^{1}/n$ with the amount of solute adsorbed being q_e, $C_e^{1/n}/q_e$ is constant at a given temperature. K_f (mg/g) is a relative indicator of adsorption capacity, while the dimensionless $^{1}/n$ indicates the energy or intensity of the reaction and suggests the favorability and capacity of the adsorbent/adsorbate system. According to the theory, n > 1 represents favourable adsorption conditions (Hokkanen et al. 2014; Mohammad, 2015).

Temkin given as **qe = A + B logCe**
equ. 3

The linear form of Temkin Isotherm can be expressed by equation
qe =RT/b lnKF + RT/b lnCe
equ. 4

Where RT/b = B (J/mol), which is Temkin constant related to heat of sorption, whereas KT (L/g) represents the equilibrium binding energy, R (8.314 J/mol/K) is the universal gas constant at T0 (k) which is absolute solution temperature **(Figures 20-22)**.

D-R isotherm linearize from as $\mathbf{lnqe = lnqs - B\varepsilon^2}$
equ. 5

The isotherm data for Pb(II) ions sorption are presented in **Table** 1. It was observed that for Azeh2, Azeh10 and Azeh-TDI, the maximum

monolayer adsorption capacity (q_m), 99 mg/g, 57 mg/g and 153 mg/g were obtained for 0.2 g, adsorbent dose respectively and these are less than the corresponding experimental adsorption capacity (qe, exp.). Therefore, the maximum monolayer adsorption capacity (q_m) obtained from the experimental data showed that Langmuir isotherm model **(Figures 13-16)** were less than the experimental adsorption capacity, indicating that the maximum amount for Pb(II) ions monolayer coverage on a unit mass of the synthesized bio-nanomaterials was exceeded by the experimental value (q_e, exp); hence the adsorption process is inconsistent with the Langmuir assumption. The above trend as shown by the values of q_m suggests the existence of multilayer adsorption phenomenon, meaning that adsorbate molecules deposit on not only the free surface of the nanomaterials, but also on already adsorbed ones. That is sorption sites accommodate more than one adsorbate molecules. From the isotherm results, Pb(II) ions showed goodness of fit with the best fitting of data for each sample by three different isotherm models in the order; Temkin>Freundlich>Langmuir for Azeh2; Temkin> Freundlich>Langmuir for Azeh10 and Langmuir>Temkin>Freundlich for Azeh-TDI. Generally, the models displayed good correlation (R^2) values for the linearize equations for the sorption process of Pb(II) ions by Azeh2, Azeh10 and Azeh-TDI samples respectively. This indicates the applicability of the tested models for sorption of Pb(II) ions. From the isotherm constants, the best isotherm that described better the adsorption Pb(II) is Freundlich isotherm model **(Figures 16-18)** which showed high K_f values, indicative of the high adsorption capacity and intensity of the nanomaterials. Therefore, k_f values for further modified samples (Azeh10 and Azeh-TDI) were found higher than H_3PO_4 acid modified sample (Azeh2) (Igwe & Abia, 2007). The Temkin equation showed goodness of fit for the adsorption of Cd(II) and Pb(II) ions, but lack the parameter describing the adsorption capacity of any given adsorbent.

The separation factor from the Langmuir isotherm model, indicative of the affinity between adsorbate and adsorbent surface, R_L, calculated for Pb(II) ions sorption process were; Azeh10 and Azeh-TDI are -0.24 and -0.08. Since, the R_L values calculated were less than 1; it therefore, indicates high favourability of the isotherm model for Pb(II)-Azeh10 and Pb(II)-Azeh-TDI. In addition, it implies that Pb(II) ions prefer to remain bound to the surface of the sample. An exception to this is the R_L values for Pb(II)-Azeh2, of 2.91 and 2.29. These values are greater than one, confirming unfavourability of the Langmuir isotherm.

The Temkin model describes the energy of adsorption (b) and (K_T) obtained in the range 11.48-15.27 and 0.612-21.51 j/mol for Pb(II) ions. This model also described the adsorption process well based on the correlation coefficient accordingly; 0.9909, 0.9993 and 0.9999 for Azeh2, Azeh10 and

Azeh-TDI. The larger the value of n the less heterogeneous is the surface of the adsorbent but with high affinity between solute and adsorbent system.

Table 1: Adsorption isotherm constants and parameters calculated for Pb(II) Adsorption
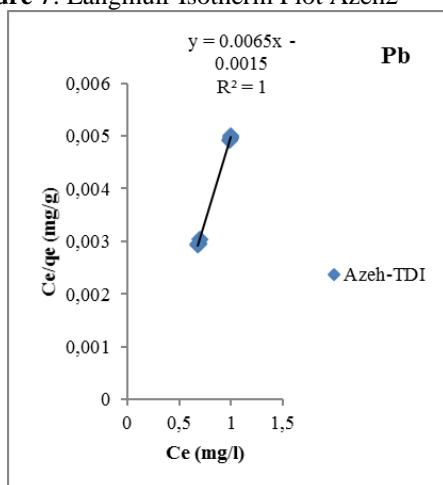
| Adsorbents	Langmuir coefficients				Freundlich coefficients			Temkin coefficients		
	q_m	-b	R_L	R^2	N	k_f	R^2	B	K_T	R^2
Azeh2	99	0.188	2.29	0.969	-2.25	148.3	0.9692	-31.13	0.1301	0.9909
Azeh10	57	1.08	-0.24	0.996	-0.79	249.7	0.9966	-14.99	0.2710	0.9993
Azeh-TDI	153	4.34	-0.08	1.00	-2.58	199.98	0.9998	-30.01	0.0900	0.9999
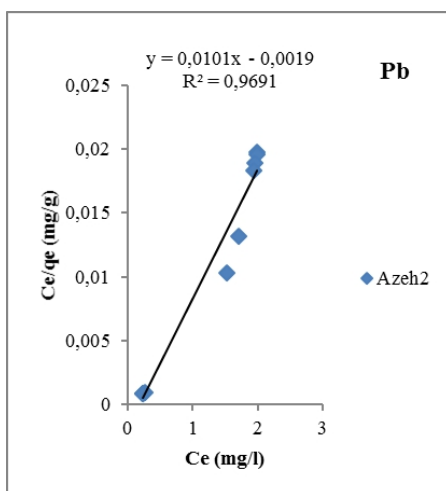
Figure 7: Langmuir Isotherm Plot Azeh2
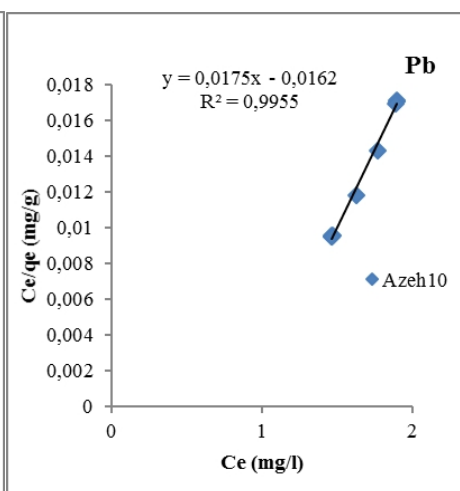
Figure 8: Langmuir Isotherm Plot Azeh10

Figure 9: Langmuir Isotherm Plot Azeh-TDI
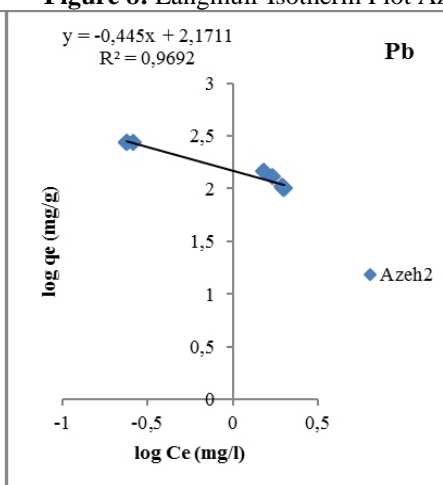
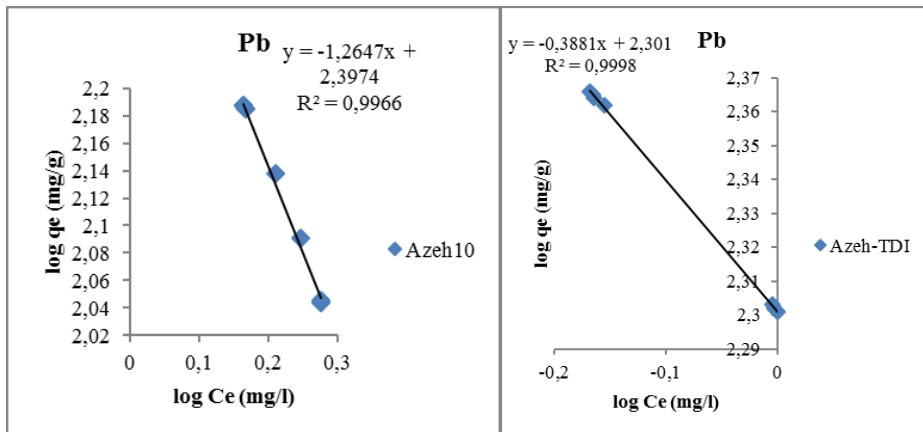**Figure 10:** Freundlich Isotherm Plot Azeh2
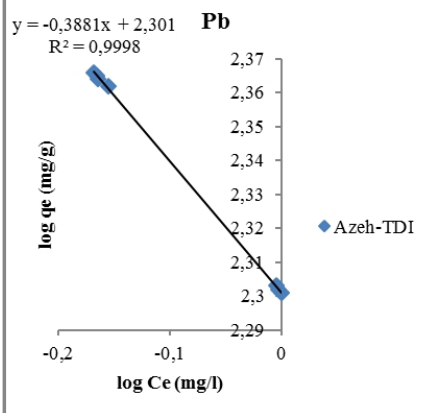
Figure 11: Freundlich Isotherm Plot Azeh10   **Figure 12**: Freundlich Isotherm Plot Azeh-TDI
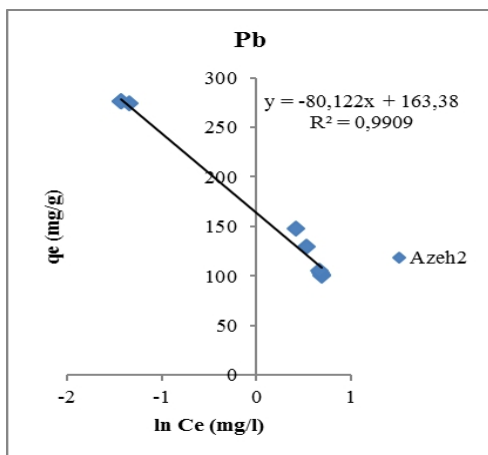
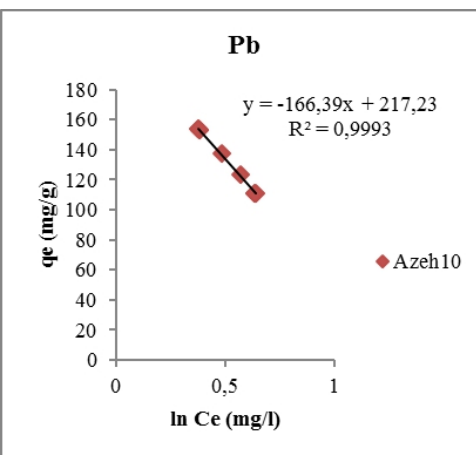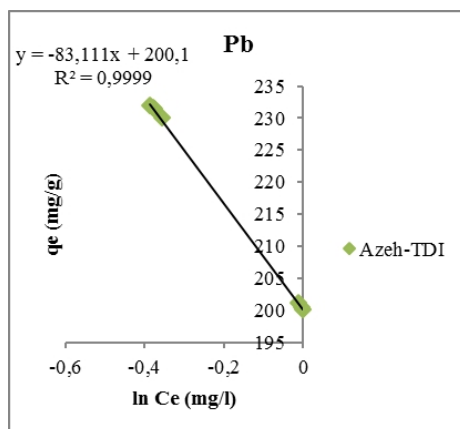**Figure 13:** Temkin Isotherm Plot Azeh2   **Figure 14:** Temkin Isotherm Plot Azeh10

Figure 15: Temkin Isotherm Plot Azeh-TDI

441

The Dubinin–Radushkevish isotherm was used in order to estimate the characteristics porosity of the synthesized bio-nanomaterials and the apparent energy of adsorption. The model is represented as; $qe = q_s \exp (- B [RT \ln (1 + 1/Ceq)]^2)$
equ.6

Where, B is related to the free energy of sorption per molecule of sorbate as it migrates from the bulk solution to the surface of the adsorbent from infinite distance and can be calculated using;

$E = 1/(2B)1/2$

equ. 7 (Itodo et al. 2010).

q_s is the Dubinin-Radushkevish isotherm constant related to the degree of sorbate sorption by the sorbent surface. The Linear form of equation (6) is given as: $\ln qe = \ln q_s – 2BRT \ln (1 + 1/Ce)$. The plots of $\ln qe$ against $RT\ln(1 + 1/Ce)$ **Figures 16-18**, yield straight lines and indicates a good fit of the isotherm to the experimental data based on the R^2. The linear regressions are shown on **Table 2.** The values of q_s, and B calculated from the intercepts and slopes of the plots are shown on **Table 2.** The apparent energy (E) of adsorption is also shown on **Table 2**.
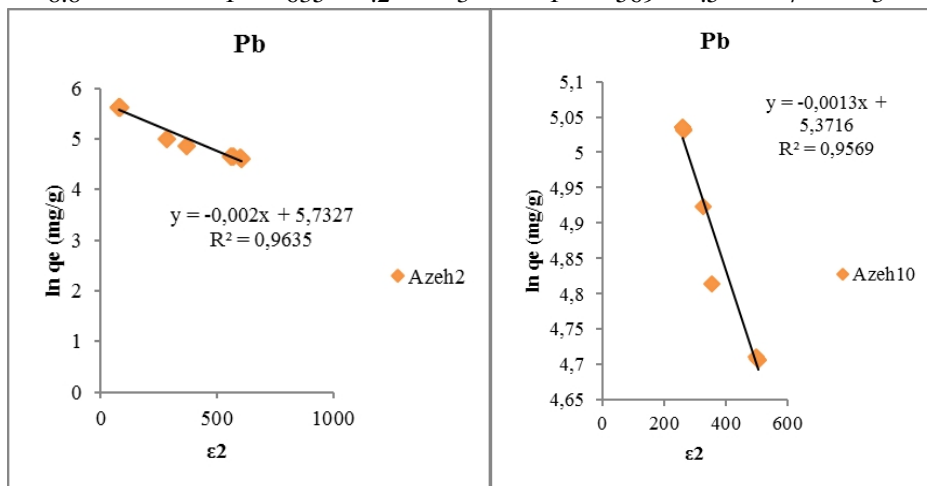
Increase in the values of q_s, is an indication of high adsorption capacity of the adsorbents. The values of q_s **Table 2** are seen to be higher for the three types of adsorbents from bio-nanomaterials. The adsorbent that was further modified with TDI, denoted as Azeh-TDI exhibited higher adsorption capacity than two others denoted as Azeh2 and Azeh10. This is linked to more possible binding sites on the surface of adsorbents resulting from chemical modification. The values of the apparent energy of adsorption shown on Table 2 depict physiosorption process (Itodo et al. 2010). This means that the Dubinin-Radushkevish isotherm gave a very good fit for the adsorption process. The mean free energy of adsorption of Pb(II) ions by the nanomaterials was positive indicating an endothermic process while high positive values obtained indicates that the adsorption process corresponds to ion exchange process (Yakout & Elsherif, 2010), and agreed with the results of pH effect.

A comparison of the coefficient of regression (R^2) for the four isotherms is shown on **Table 3.** For the Langmuir isotherm, the range of R^2 is 0.972-0.999 for Cd, with an average value of 0.9867. For Pb, the range is 0.969-1.000 with an average of 0.9883. For Freundlich isotherm, the range is 0.9615-0.9970 with an average value of 0.9836 for Cd and 0.9692-0.9998 with an average value of 0.9885 for Pb. The range for the Temkin isotherm is 0.9546-0.985 with an average value of 0.9797 for Cd and 0.9909-0.9999 with an average of 0.9965 for Pb. For the Dubinin-Radushkevish isotherm, the range of R^2 value for Cd is 0.9744-0.9991, with an average value of 0.9883. For the Pb the range is 0.9569 to 1.000 with an average value of

0.6735. Therefore, based on the correlation coefficient of regression R^2, one can say that the isotherms are appropriate in their own merits in describing the potential of the synthesized nanomaterials for removal of Pb(II) ions in solution. We can also conclude from the average values of R^2 for each metal ion that the order of fitness is in decreasing order; Temkin>Freundlich>Langmuir>D-R, for Pb(II) ion adsorption process while for Cd, the order is D-R>Langmuir>Freundlich>Temkin. The values of B calculated were negative because the slopes of their plots were negative, similar to those reported (Itodo et al. 2010).

Table 3: Dubinin-Radushkevish (D-R) Coefficients obtained from kinetic data

Metal ions	Azeh2				Azeh10				Azeh-TDI			
	q_s mg /g)	-b (mol^2 /jol^2	E KJ/ mol	R^2	q_s (mg /g)	-b (mol^2 /jol^2	E (KJ/ mol)	R^2	q_s (mg /g)	-b (mol^2 /jol^2	E KJ/ mol	R^2
Pb	308.8	0.002	15.81	0.9635	215.2	0.001	19.63	0.9569	365.5	0.003	11.67	1.000

Figure 16: Dubinin-Radushkevish (D-R) plot   **Figure 17**: Dubinin-Radushkevish (D-R) plot
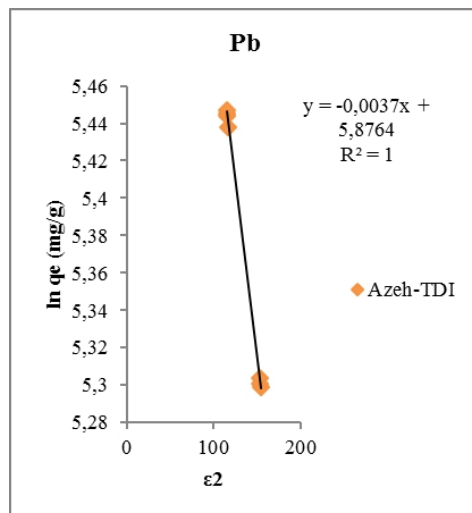
**Figure 18**: Dubinin-Radushkevish (D-R) plot

Adsorption Kinetics

The study of the mechanism of adsorption process of Pb(II) ions, sorption data for Azeh2, Azeh10 and Azeh-TDI samples at 300 K and pH 6.0 are tested for kinetic modelling by linear regression plots (**Figures 19-22**). Four kinetic models (pseudo-second-order, Power function, Intra-particle diffusion and simple Elovich model (**Figures 19-22**), were used to fit the experimental data are shown in **Table 4**. The pseudo-second order kinetic model given as $^{t}/q_{t} = (^{1}/K_{2}q_{e}^{2}) + (^{1}/q_{e})t$ **equ. 8**

This described the adsorption data for Pb ions sorption by Azeh2, Azeh10 and Azeh-TDI best with good correlation coefficients in the range of 0.9949-0.9999 for Pb(II). The plot of t/q_{t} Vs t of experimental data showed good degree of agreement with q_{e}, calculated. The equilibrium rate constants Pb(II) sorption increased in the order; Azeh2<Azeh-TDI<Azeh10. The applicability of pseudo second order model showed that the rate limiting step is chemisorptions involving valence forces cause by sharing or exchange of electrons between sorbent and sorbate (Kushwaha et al. 2008). On the other hand, the power function model in the linear form as (**logq_t = logk_p + Vlogt, equ. 9**) fairly fits the kinetic data better than intra-particle diffusion model with coefficient of regression in the range, $0.7642<R^{2}<0.8925$ and $0.3841<R^{2}<0.7564$. The constant "v" was in the range 0.0398-0.2348. The value of v, was less than 1, which indicates that the power function described the time dependent of Pb adsorption on the synthesized nanomaterials. This observation is similar to that reported on Cr(VI) adsorption by synthetic hematite nanoparticles (Adegoke et al. 2014). The Elovich equation showed appreciable good correlation coefficients for the adsorption process in the range of 0.7603 – 0.8939. The initial sorption rate for Pb by modified

samples was quite high and followed the order; Azeh-TDI>Azeh10>Azeh2. The reason for this is attributed to the heterogeneous surface of the adsorbents, caused by new functional species attached to nanomaterials resulting from modification. Additionally, the presence of new functional species enhanced chemisorption of Pb(II) ions in solution. Elovich equation is useful for describing chemisorption on a highly heterogeneous adsorbent (Adegoke et al. 2014).

**Table 4.** Adsorption kinetics Constants for Pb (II) adsorption

	Pseudo-Second-Order			Power function			Intra-particle diffusion			Elovich		
Sample	K_2 (g/mg/min)	q_e (mg/g)	R^2	K_p	V	R^2	Kid	I (mg/g)	R^2	A	b	R^2
Azeh2	8.794×10^{-5}	285.70	0.9949	57.2	0.2348	0.8669	6.2691	95.59	0.7564	-2.603	40.927	0.8336
Azeh10	7.249×10^{-4}	156.25	0.9999	88.3	0.0858	0.8925	1.4462	113.1	0.6997	80.431	11.297	0.8939
Azeh-TDI	6.848×10^{-4}	232.56	0.9999	178.1	0.0398	0.7642	0.7979	207.86	0.3841	176.49	8.156	0.7603
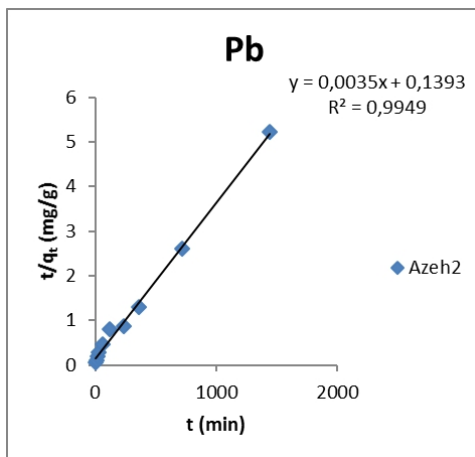
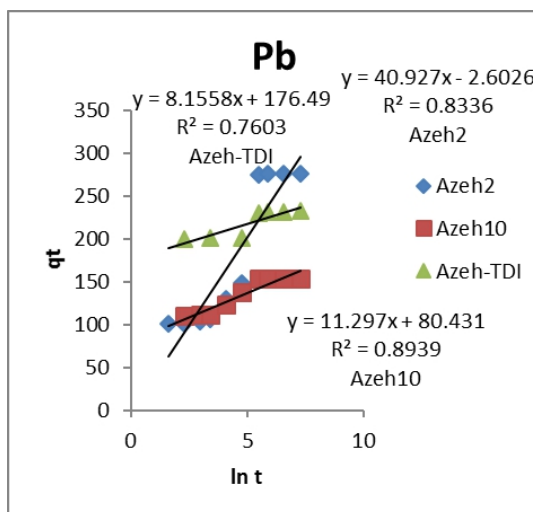**Figure 19:** Pseudo-Second Order Kinetics Plot Azeh2
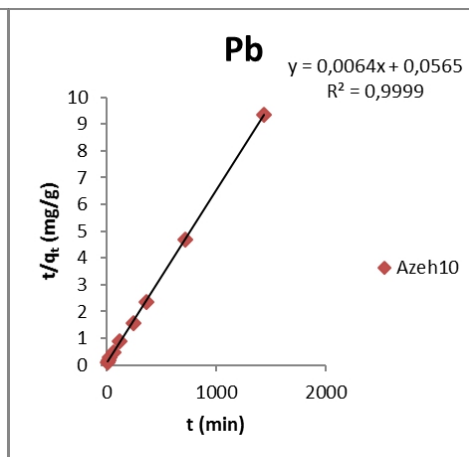
Figure 20: Pseudo-Second Order Kinetics Plot Azeh10
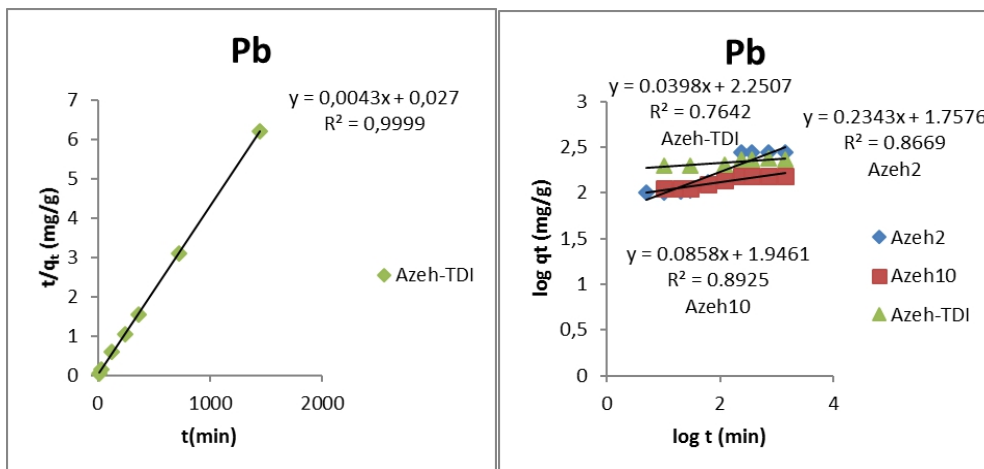
Figure 21: Pseudo-Second Order Kinetics Plot Azeh-TDI

Figure 22: Power function Kinetics Plot

Figure 22: Elovich plot Intra-particle diffusion

Intra-Particle Diffusion Model

The structure of adsorbents and their interactions with diffusion substance influences the rate of transport. This model was used to predict the nature of the synthesized adsorbents and mode of transport process of Pb(II) ions from the bulk of the solution to the solid phase. Adsorbent may be in the form of porous barriers and solute movement by diffusion from one fluid body to the other by virtue of concentration gradient (Itodo et al. 2010). In a well stirred batch adsorption system, the intra-particle diffusion model has been used to describe the adsorption process occurring on a porous adsorbent (Itodo et al. 2010). A plot of the amount of sorbate adsorbed, qt (mgg^{-1}) and the square root of the time, gives the rate constant (slope of the plot)

(**Figures 23-25**). It is calculated by using the intra-particle diffusion model given as equation 8 (Mohammad, 2015; Itodo et al. 2010).

qt = kid t$^{(1/2)}$ + I

kid (mgg^{-1} min$^{-1(1/2)}$) is a measure of diffusion coefficient. I = intraparticle diffusion constant i.e. intercept of the line (mgg^{-1}). The constant I, is directly proportional to the boundary layer thickness.

The plots (**Figures 23-25**) for these analyses revealed three step linear stages occurring during Pb(II) uptake. The first one corresponding to fast uptake of sorbate showed a closely packed consecutive arrangement and the line in the initial stage does not pass through the origin. This stage confirms that metal ion uptake was dominated by film diffusion than it does for the intra-particle diffusion process (Ho et al. 2000; Itodo et al. 2010; Yakout & Elsherif, 2010; Liu et al. 2012). In the second stage, it was observed that the adsorption process of Pb by the adsorbents speeds up in varied manner indicating some interruptions had occurred during diffusion of sorbate molecules into the micropores with wider pore width within the sorbent (Itodo et al. 2010). The third stage revealed a steady and slow diffusion of Pb(II) ions into the micropore volume of the adsorbents. This confirms the microporous nature of the synthesized adsorbents and this further supports the results obtained from BET with micropore volume the range of 0.01427–0.07939 cm^3/g. The steady and slow diffusion was indicative of the fact that the pore volume was exhausted. According to (Biyan et al. 2009), adsorption controlled by the intra-particle model is due to the preferential adsorption of sorbate in the micropore of the adsorbent. From the results of the intra-particle model, it is evidence that, intra-particle diffusion of sorbate is neither the rate controlling nor the rate limiting step here, since the plots do not pass through the origin. In addition, there may be some degree of boundary layer control due to other kinetic processes working simultaneously during adsorption or one could say that the mechanism of Pb adsorption is complex and both surface sorption and intra-particle diffusion is rate determining step (Ho et al. 2000; Kushwaha et al. 2008; Yakout, E. Elsherif, 2010; Liu et al. 2012). The intra-particle diffusion rate constant, Kid, values obtained from the slope of the straight-line portions of plot of **qt versus t$^{1/2}$** for various adsorbents as shown in **Table 5**. The correlation coefficients (R^2) for the intra-particle diffusion model are between 0.3841-0.7564 for Pb(II) ions at 300K. It was observed that intra-particle rate constant values (Kid) and (I), varied for the adsorbents in the order; Kid = 4.3317>1.5755>1.044 (mgg^{-1}min$^{-1(1/2)}$) for Azeh2, Azeh10 and Azeh-TDI; I = 199.91>112.19 >108.4 for Azeh-TDI, Azeh10 and Azeh2. The results showed that Azeh2 is seems more porous than others based on the rate constant Kid, and the adsorbent with the least surface porosity is Azeh-TDI, but exhibited high value of I, indicative of the nature (large) of

the boundary layer. According to (Liu et al. 2012), increase in the values of Kid and I relates to increase in thickness of boundary layer of the adsorbents. In this study, the order of increase in thickness of the boundary layer is I = 199.91>112.19>108.4 for Azeh-TDI, Azeh10 and Azeh2 for Pb adsorption, reflecting the resistance to external mass transfer. This therefore, favoured internal mass transfer (Liu et al. 2012). The results showed large values of intercept which is indicative of the large contribution of surface adsorption at the initial adsorbate concentration. Intra-particle studies for the adsorption of Pb(II) ions onto sawdust gave large values of intercept, which suggests that high initial concentration has relatively strong tendency for surface adsorption have been reported (Jihyun et al. 2008).
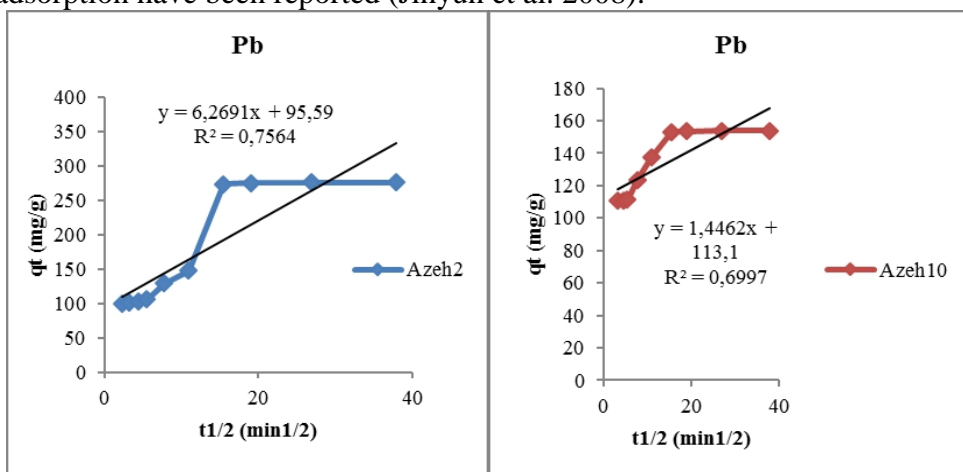

Figure 23: Intra-particle diffusion plot   **Figure 24:** Intra-particle diffusion plot
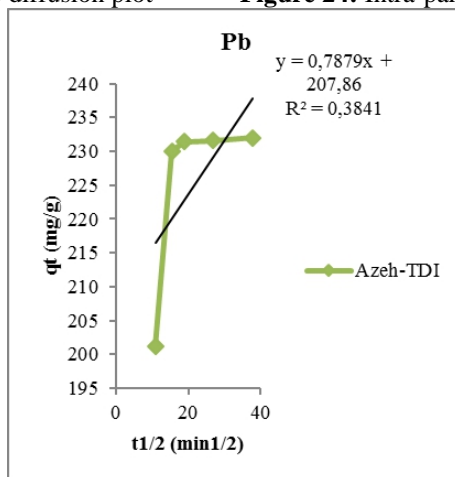

Figure 25: Intra-particle diffusion plot

Diffusion coefficients for the intra-particle transport of Pb(II) ions within the pores of nanomaterial particles have been calculated by employing equation (9)

448

Di = 0.03 X r^2/t$_{1/2}$
equ. 9 (Yakout & Elsherif, 2010).

Where **Di** is the diffusion coefficients with the unit **cm^2/s; t$_{1/2}$** is the time (s) for half-adsorption of Pb(II) ions and r is the average radius of the adsorbent particle in cm. Assuming spherical geometry of the sorbents. The value of r (average radius) was calculated from pore radius of the adsorbents obtained from BET analysis (15.10 and 15.30 Armstrong) as 1.51 X 10^{-7}and 1.53 X 10^{-7} cm for Azeh2, Azeh-TDI and Azeh10 respectively. According to (Karthikeyan et al. 2010) for film diffusion to be rate-determining step, the value of the film diffusion coefficient, **D$_f$**, should be in the range 10^{-6} - 10^{-8} cm^2/ sec. If pore diffusion were to be the rate limiting, the pore diffusion coefficient, **Dp**, should be in the range 10^{-11}- 10^{-13} cm^2/ sec.

Table 5: Diffusion coefficient for intra-particle transport of Pb (II) ions

Azeh2	Azeh-TDI	Azeh10
Diffusion coefficients (cm^2/s)		
3.02 X 10^{-11}	3.02 X 10^{-11}	3.06 X 10^{-11}
1.51 X 10^{-11}	1.51 X 10^{-11}	1.53 X 10^{-11}
7.55 X 10^{-12}	7.55 X 10^{-12}	7.65 X 10^{-12}
5.03 X 10^{-12}	5.03 X 10^{-12}	5.1 X 10^{-12}
2.51 X 10^{-12}	2.51 X 10^{-12}	2.55 X 10^{-12}
1.258 X 10^{-12}	1.258 X 10^{-12}	1.275 X 10^{-12}
6.29 X 10^{-13}	6.29 X 10^{-13}	6.375 X 10^{-13}
4.194 X 10^{-13}	4.194X10^{-13}	4.25 X 10^{-13}
2.097 X 10^{-13}	2.097 X 10^{-13}	2.125 X 10^{-13}
1.049 X 10^{-13}	2.097 X 10^{-13}	1.063 X 10^{-13}

The results of the diffusion coefficients calculated using the above formula in order to predict the nature of diffusion mechanism of Pb sorption process, showed that the order of diffusion coefficients was 10^{-11} - 10^{-13} cm^2 / sec which indicates that pore diffusion has some significant influence in the rate determining step. This is in agreement with the long time taken for the adsorption process to attain equilibrium (12h) as reported in literature (Paritam et al. 2004). In addition, the values of the internal diffusion coefficient, *Di*, shown in Table (5) are within the magnitudes reported in literature, specifically for chemisorption system (10^{-5} to 10^{-13} cm^2/s) (Yakout & Elsherif, 2010).

Deduction of Kid In Terms of % Sorption

The Weber and Morris equation for prediction of the intra-particle diffusion in terms of percent sorption of sorbate in solution by adsorbent

according to (Itodo et al. 2010) was used in this analysis as presented in equation 10a and 10b.

R = kid (t)^a

equ.   (10a)

Linearized form of the equation is given as

log R = log kid + a log (t)

equ.   (10b)

Where R = percent of sorbate adsorbed, t = contact time (minutes), a = gradient of linear plot. The value of 'a' depicts the adsorption mechanism. kid is the intra-particle rate constant (time^{-1}). It is taken as rate factor i.e. percent of sorbate adsorbed per unit time ($mgg^{-1}min^{-1(1/2)}$).

According to reports (Yakout & Elsherif, 2010), higher values of kid are indicators of an enhancement rate of adsorption and improved bonding between sorbate and sorbent particles. This model was used to analyse further the experimental data **(Figure 26)**. The application of the model gave a goodness of fit with correlation coefficients (R^2) in the order; 0.8922> 0.8677>0.7614 for Pb (II) ions (Azeh10>Azeh2>Azeh-TDI) and a value of "a" which is less than unity in the range of 0.0378 - 0.2343 and the intra-particle diffusion rate constant, kid for each adsorbent is 59.79/Azeh-TDI, 29.41/Azeh10 and 19.07/Azeh2 respectively. The enhanced rate of adsorption is linked to improved bonding between sorbent-sorbate systems. The kid value with estimation based on percentage uptake of Pb ions is far less related to that which was based on qt and t$^{1/2}$ plots. This suggests that sorption mechanism is not intraparticle diffusion control, but a combination of mechanisms.

Irrespective of the linearity (high R^2 value) of the intra-particle diffusion plot, the sorption mechanism assumes intra-particle diffusion if the following conditions are satisfied:

(i) High R^2 values to ascertain applicability, (ii) Straight line which passes through the origin for the plot area qt vs. t$^{1/2}$, (iii) Intercept I < 0.

According to (Hameed, 2009), a validity test which deviates from (ii) and (iii) above shows that the mode of transport is affected by more than one adsorption mechanism.
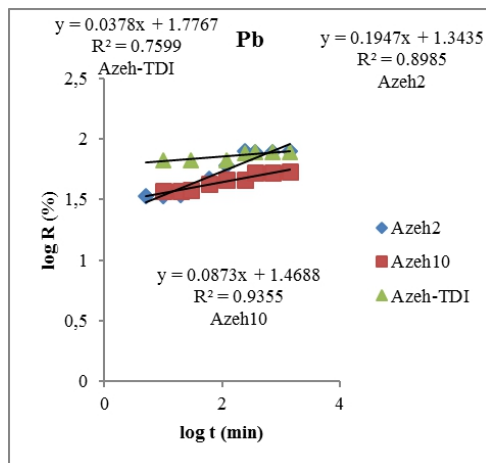
**Figure 26:** logR vs log t based on % uptake of Pb per unit time

Adsorption Thermodynamics

Thermodynamics parameters for the adsorption of Pb (II) ions onto Azeh2 and Azeh-TDI, samples are presented in **Table 6.** The data showed that change in enthalpy (ΔH) of the adsorption process by Azeh-TDI has a negative value of -12.812 X 10^3 KJ/mol for Pb(II) ions. This indicates that the Azeh-TDI was exothermic. In addition, the entropy (ΔS) for the system increased with values greater than zero (8.6 X 10^1 and 8.5 X 10^1 KJ/mol). This gave rise to negative values of change in Gibbs (ΔG) free energy, 15.364 X 10^3 KJ/mol. This confirmed the feasibility and spontaneous nature of the sorption process. As reported in literature, low negative value of change in enthalpy is an indication that physical adsorption is among the mechanism of the adsorption process (Mohammad, 2015). This suggests a decrease in adsorbate concentration in solid-solution interface, indicating the increase in sorbate concentration onto the solid phase. This was a normal consequence of the physical adsorption phenomenon, which took place through electrostatic interactions as reported (Goswami & Ghosh, 2005). The enthalpy change for Pb adsorption by Azeh2 was positive with a ΔH = 12.7071 X 10^4 KJ/mol and change in ΔG = 12.7384 X 10^4 KJ/mol. This indicates that the adsorption process was endothermic and non-spontaneous. According to (Zeng, 2014), negative values imply a decrease in disorder at the sorbent/solution interface. The Gibbs free energy for Pb ions adsorption process by the Azeh2 and Azeh-TDI was negative and decreased with increasing temperature from 310 – 360 K. This observation implied that the adsorption process is thermodynamically favoured and will proceed spontaneously in the forward direction to form more products. This may be responsible for the high uptake of metal ion from their solutions by the samples with increasing temperature. These opposite thermal natures have also been found for As (V) and As (III) adsorption on some mixed oxides
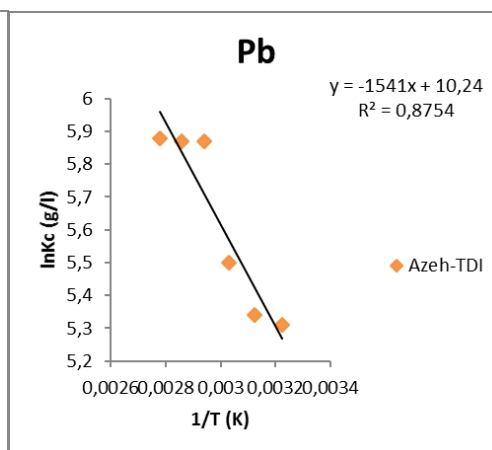
such as red mud (Zeng, 2014), where the adsorption of As (V) was endothermic and the adsorption of As (III) was exothermic. The positive $\Delta S°$ value reflects the affinity of the adsorbent material for Pb (II) ions and suggests possible structural changes in the Pb species and the adsorbent (Zeng, 2014). Furthermore, the positive value of $\Delta S°$ shows the increasing randomness at the solid/liquid interface during Pb (II) ions adsorption by the adsorbent (Ho et al. 2000). The implication of the difference in the thermodynamic parameters of Pb (II) ions is that the surface adsorption of anionic species might be different from that of cationic species on the nanomaterials. The linear plots **(Figures 27 and 28)** showed that Azeh-TDI sample had a better representation of the data with regression coefficient 0.8754 **(Figure 28)**.

Table 6. Thermodynamic parameters for the adsorption of Pb (II)
Onto Azeh2 and Azeh-TDI sample

Sample	Metal	ΔG (kJ/mol)	ΔS (kJ/mol)	ΔH (kJ/mol)
Azeh-TDI	Pb	-15.364×10^3	8.5×10^1	-12.812×10^3
Azeh2	Pb	12.7384×10^4	-3.12×10^2	12.7071×10^4
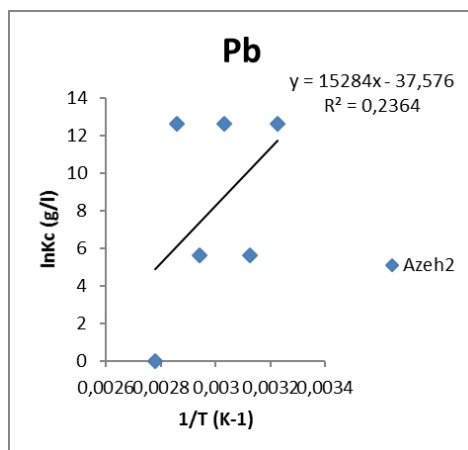
Figure 27: Thermodynamic plot Azeh2   **Figure 28:** Thermodynamic plot Azeh-TDI

Conclusion

In recent times, there has been increasing interest in the use of biopolymers and green synthesis routes for cost effective adsorbents as better alternative for biosorption of metal ions in aqueous solutions. Nanomaterials of cellulose origin have been found to exhibit high performance in almost all fields of science and engineering due to their robust chemical and mechanical properties compared to their bulk counterparts. In this study, the synthesized nanoparticles from cellulose origin showed high adsorption capacities and removal efficiency for Pb(II) ions in aqueous solution. This study showed that phosphoric acid and CA synthesized nanoparticles were efficient for lead removal. Modification of phosphorylated nanoparticle

using toluene diisocyanate (TDI) showed higher removal capability for lead uptake. This was due probably to more number of functionalities introduced unto the surface of phosphorylated nanoparticles. Enhanced adsorption capacity for Pb(II) ions was observed for the synthesized nanoparticles. The negative ΔG and ΔH implied that, the adsorption process of Pb(II) by Azeh-TDI was exothermic while Pb^{2+} adsorption by Azeh2 (H_3PO_4-modified) was endothermic in nature due to positive ΔG and ΔH values. This indicates that the adsorption process for Pb(II) ions onto Azeh-TDI was feasible and spontaneous. Pore diffusion had significant influence in the rate determining step for the adsorption of Pb(II) ions. Hence, the synthesized nanoparticles have the potentials for applications for treatment of water/wastewater laden with Pb(II) contamination.

References:
1. Abdus-Salam, N., & Adekola, F. A. (2005). The influence of pH and adsorbent concentration on adsorption of lead and Zinc on a natural goethite. African Journal of Science and Technology (AJST), *Science and Engineering Series* 6(2), 55 – 66.
2. Asadi, F., Shariatmadari, H., & Mirghaffari, N. (2008). Modification of rice hull and sawdust sorptive characteristics for removal of heavy metals from synthetic solutions and wastewater. *Journal of Hazardous Materials*, 154, 451–458 (2008).
3. Azeh, Y., Tanko, M. U., Sani, S. D. M. (2011). Chemical modification of microcrystalline cellulose: Improvement of barrier surface properties to enhance surface interactions with some synthetic polymers for biodegradable packaging material processing and applications in textile, food and pharmaceutical industry. *Advances in Applied Science Research*, 2 (6), 532-540.
4. Anna, K., Maria, H., Yulia, L., Anatoliy, K., Anatoliy, P., & Tatiana, M. (2012). Oxo-biodegradability of polyethylene blends with starch, cellulose and synthetic additives. *Chemistry and Chemical Technology*, 6 (4), 405-413.
5. Atanu, B., Badal, C. S., Lawton, J. W., Shogren, R. L., & Willett, J. L. (2006). Process for obtaining cellulose acetate from agricultural by-products. *Carbohydrate Polymers*, 64, 134-137.
6. Anuj, K., Yuvraj, S. N., Veena, C., & Nishi, K. B. (2014). Characterization of cellulose nanocrystals produced by acid-hydrolysis from sugarcane bagasse as agro-waste. *Journal of Materials Physics and Chemistry,* 2 (1), 1-8.
7. Adebayo, G. B., Abdus-salam, N., Elelu, S. A. (2014). Adsorption of lead (II) ions by activated carbon prepared from different parts of *Jatropha Curcas* Plant. *Ilorin Journal of Science,* 1(1), 28 – 49.

8. Adegoke, H. I., Adekola, F. A., Fatoki, O. S., & Ximba, B. J. (2014). Adsorption of Cr (VI) on Synthetic Hematite (α-Fe_2O_3) Nanoparticles of Different Morphologies. *Korean J. Chem. Eng.,* 31(1), 142-154. DOI: 10.1007/s11814-013-0204-7.

9. Andal, N. M., & Gohulavani, G. (2013). Sorption kinetics and equilibrium studies on the removal of toxic Cr(VI) ions employing modified Indian almond nut shells. *Journal of Energy Technologies and Policy,* 3, 11, 153-164.

10. Bhatnagar, A., & Minocha, A. K. (2006). Conventional and non-conventional adsorbents for removal of pollutants from water. *Carbohydrate Polymers,* 77, 142–149.

11. Biyan, J., Fei, S., Hu, G., Zheng, S., Zhang, Q., & Xu, Z. (2009). Adsorption of methyl tert-butyl ether (MTBE) from aqueous solution by porous polymeric adsorbent. *Journal of Hazard Material.* 161 (1), 81-87.

12. Barakat, M. A. (2011). New trends in removing heavy metals from industrial wastewater. *Arabian Journal of Chemistry*, 4, 361–377.

13. Dada, A. O., Ojediran, J. O., & Abiodun, P. O. (2013). Sorption of Pb^{2+} from aqueous solution unto modified rice husk: Isotherms studies. *Advances in Physical Chemistry*, 2013, Article ID 842425, 6 pages.

14. Edokpayi, J. N., Odiyo, J. O., Msagati, T. A. M., & Popoola, E. O. (2015). Novel Approach for the removal of lead(II) Ion from wastewater using mucilaginous leaves of diceriocaryum eriocarpum plant. *Sustainability*, 7, 14026-14041.

15. Filpponen, I. (2009). The synthetic strategies for unique properties in cellulose nanocrystals materials (Published doctoral thesis) North Carolina State University, Raleigh, North Carolina.

16. Farre, A. L. (2015). (Master of Science Thesis) Chalmers University of Technology Gothenburg, Sweden.

17. Fu, F., & Wang, Q. (2011). Removal of heavy metal ions from wastewaters. *Journal of Environmental Management*, 92, 407-418.

18. Gurgel, L. V. A., & Gil, L. F. (2009). Adsorption of Cu (II), Cd (II), and Pb (II) from aqueous single metal solutions by succinylated mercerized cellulose modified with triethylenetetramine. *Carbohydrate Polymers*, 77, 142–149.

19. Gadd, G. M. (2009). Biosorption: critical review of scientific rationale, environmental importance and significance for pollution treatment. *J. Chem Technol Biotechnol*., 84, 13–28.

20. Goswami, S. U., & Ghosh, C. (2005). Studies on adsorption behaviour of Cr (vi) onto synthetic hydrous stannic oxide. *Water SA* 31 (4), 597-602.

21. Hubicki, Z., & Kołodynska, D. (2012). Selective removal of heavy metal ions from waters and waste waters using ion exchange methods Intech., 193-240.
22. Hokkanen, S., Repo, E., & Suopajärvi, T. (2014). Adsorption of Ni(II), Cu(II) and Cd(II) from aqueous solutions by amino modified nanostructured microfibrillated cellulose. *Cellulose*, 21, 1471–1487.
23. Hubbe, M. A., Hasan, S. H., & Ducoste, J. J. (2011). Cellulosic substrates for removal of pollutants from aqueous systems. Metals. BioResources, 6, 2161–2287.
24. HO, Y. S., Ho, Ng, J. C. Y., & McKay, G. (2000). Kinetics of Pollutant sorption by biosorbents: Separation and purification methods, 29(2), 189–232.
25. Hameed, B. H. (2009). Evaluation of papaya seed as a non conventional low cost adsorbent for removal of MB. Hazardous materials.162, 939-944.
26. Igwe, J. C., & Abia, A. A. (2007). Adsorption isotherm studies of Cd (II), Pb (II) and Zn (II) ionsbioremediation from aqueous solution using unmodified and EDTA-modified maize cob, 32, número 1.
27. Itodo, A. U., Abdulrahman, F. W., Hassan, L. G., Maigandi, S. A., & Itodo, H. U. (2010). Intraparticle diffusion and intraparticulate diffusivities of herbicide on derived activated carbon. Researcher, 2(2), 74-86.
28. Jain, P. (2014). Biosorption of hexavalent chromium from aqueous medium with the antibiotic residue (A Synopsis for doctoral thesis) Deemed University, Dayalbagh Agra-282 005.
29. Jonas, B. (2014). Investigation of bacterial cellulose as a carbon fiber precursor and its potential for piezoelectric energy harvesting (Published M. Sc. thesis) Cornell University.
30. Jabbar, A. M., & Timell, T. E. (1960). Isolation and characterization of cellulose from the inner bark of white birch (Betula Papyrifera). Can. J. Chem., 38, 1191-1198 (1960).
31. Jihyun, L., Hee-Man, K., Lee-Hyung, K., & Seok-Oh, K. (2008). Removal of Heavy Metals by Sawdust Adsorption: Equilibrium and Kinetic Studies.Environ. Eng. Res. 13 (2), 79-84.
32. Khezami, L., Bessadok-Jemai, A., Dauij, A. O., & Amami, E. (2012). Individual and competitive adsorption of Lead(II) and Nickel(II) ions by chemically activated carbons. International Journal of Physical Sciences, 7 (46), 6075-6081.
33. Kushwaha, S., Sodaye, S., & Padmaja, P. (2008). Equilibrium, kinetics and thermodynamic studies for adsorption of Hg (II) on palm shell powder. World Academy of Science, Engineering and Technology 19, 597-603.

34. Karthikeyan, S., Sivakumar, B., & Sivakumar, N. (2010). Film and pore diffusion modeling for adsorption of reactive red 2 from aqueous solution on to activated carbon prepared from bio-diesel industrial waste, E-Journal of Chemistry, 7 (S1), S175-S184.

35. Liu, P. (2015). Adsorption behaviour of heavy metal ions from aqueous medium on nanocellulose (Published doctoral thesis) Lulea University of Technology Lulea, Sweden.

36. Li, X., Tang, Y., Xuan, Z., Liu, Y., & Luo, F. (2007). Study on the preparation of orange peel cellulose adsorbents and biosorption of Cd^{2+} from aqueous solution Separation and Purification Technology 55, 69–75.

37. Liu, L. Liu, J. Li, H. Zhang, H. Liu, J., & Zhang, H. (2012). Equilibrium, kinetics and thermodynamics studies of lead (II) biosorption on sesame leaf. Bio-Resources, 7 (3), 3555-3572.

38. Mautner, A., Maples, H. A., Kobkeatthawin, T., Kokol, V., Karim, Z., Li, K., & Bismarck, A. (2016). Int. J. Environ. Sci., Technol. DOI 10.1007/s13762-016-1026-z.

39. Mehmet, E. A., & Şukru, D. (2006). Removal of heavy metal ions using chemically modified adsorbents. J. Int. Environmental Application & Science, 1 (1-2), 27-40.

40. Mudasir, A. S., Swami, B. L., & Ikram, S. (2015). Adsorption of heavy metal ions: Role of Chitosan and cellulose for water treatment IJP, 2(6), 280-289.

41. Mohammad, Y. S. (2015). Performance evaluation of treated rice husk activated carbon in water treatment and removal of phenol (Unpublished doctoral thesis) Ahmadu Bello University Zaria, Nigeria.

42. Onundi, Y. B., Mamun, A. A., Al Khatib, M. F., & Ahmed, Y. M. (2010). Adsorption of copper, nickel and lead ions from synthetic semiconductor industrial wastewater by palm shell activated carbon. Int. J. Environ. Sci., Tech., 7 (4), 751-758.

43. Olaniyi, I. (2011). Adsorption study of Cr(VI) and Pb(VI) from aqueous solution using animal charcoal derived from cow bone (Published master of science thesis) Ahmadu Bello University, Zaria, Nigeria.

44. Peng, B. L., Dhar, N., Liu, H. L., & Tam, K. C. (2011). Chemistry and applications of nanocrystalline cellulose and its derivatives: A nanotechnology perspective. Can. J. Chem. Eng. 9999 (1–16).

45. Paritam, K. D., Ajay, K. R., Virender, K. S., Frank, J. M. (2004). Adsorption of arsenate and arsenite on titanium dioxide suspensions. Journal of Colloid and Interface Science 278, 270–275.

46. Quintelas, C., Rocha,R., Silva, B., Fonseca, B., Figueiredo, H., & Tavares, T. (2009). Chemical Engineering Journal, 149, 319–324.

47. Rodionova, G., Lenes, M., Eriksen, O., Gregersen, O., & Berichte, L. (2009). Surface chemical modification of microfibrillated cellulose: Improvement of barrier properties for packaging applications, 87, 38-46.

48. Robert, M. J., Ashlie, M., John, N., John, S., & Jeff, Y. (2011). Cellulose nanomaterials review: structure, properties and nanocomposites. Chem. Soc. Rev., 40, 3941–3994.

49. Rosa, M. F., Medeiros, E. S., Malmonge, J. A., Gregorski, K. S., Wood, D. F., Mattoso, L. H. C., Glenn, G., Orts, W. J., & Imam, S. H. (2010). Cellulose nanowhiskers from coconut husk fibers: Effect of preparation conditions on their thermal and morphological behaviour. Carbohydrate Polymers 81, 83–92.

50. Sciban, M., Klasnja, M., & Skrbiæ, B. (2008). Removal of Cd(II), Cr(VI), Fe(III) and Ni(II) from aqueous solutions by an E. coli biofilm supported on kaolin. Desalination, 229, 170–180.

51. Stephen, J. E., (2010). Cellulose nanowhiskers: Promising materials for advanced applications. DOI: 10.1039/c0sm00142b

52. Sewwandi, B. G. N., Vithanage, M., Mojood, N. I. M., Kawomoto, K., & Hamamoto, S. (2012). Removal of heavy metals from wastewater using Agricultural waste Materials EE2 Seminar, Water and Environment in Asia`s Developing Communities.

53. Shatkin, J. A., Wegner, T. H., Bilek, E. M., & Cowie, J. (2014). Market projections of cellulose nanomaterial-enabled products − Part 1: Applications. Tappi Journal, 13 (5), 1-8.

54. Sadaf, S., Bhatti, H. N., Ali, S., & Rehman, K. (2013). Removal of indosol turquoise FBL dye from aqueous solution by bagasse, a low cost agricultural waste: batch and column study. Desalin. Wat. Treat. 2013.780985.

55. Suopajarvi, T. (2015). Functionalized nanocelluloses in wastewater treatment applications (Published doctoral thesis) University of Oulu, Oulu.

56. Thouraya, B., Isabel, V., & Abdelmottaleb, O. (2013). Comparative study of bivalent cationic metals adsorption Pb(II), Cd(II), Ni(II) and Cu(II) on olive stones chemically activated carbon. J. Chem. Eng. Process Technol., 4:4.

57. Wojnarovits, L., Foldvary, C. S. M., & Takacs, E. (2010). Radiation-induced grafting of cellulose for adsorption of hazardous water pollutants: Radiation Physics and Chemistry, 79, 848–862.

58. Xining, S., Jingjing, M., Zengqiang, Z., & Zhiyong, Z. (2015). Advance Journal of Food Science and Technology, 7(2), 120-128.

59. Xiaolin, Y., Shengrui, T., Maofa, G., Lingyan, W., Junchao, Z., Changyan, C., & Weiguo, S. (2012). Biosorption: critical review of scientific rationale, environmental importance and significance for pollution treatment J. Environmental Sciences, 24, 1-26.

60. Yusoff, S. N. M., Kamari, A., Putra, W. P., Ishak, C. F., Mohamed, A., Hashim, N., & Isa, I. M. D. (2014). Removal of Cu(II), Pb(II) and Zn(II) ions from aqueous solutions using selected agricultural wastes: Adsorption and characterisation studies. Journal of Environmental Protection, 5, 289-300. PAPER

61. Yanxia, Z., Tiina, N., Carlos, S., Julio, A., Ingrid, C. H., & Orlando, J. R. (2013). Cellulose Nanofibrils: From strong materials to bioactive surfaces. J. Renew. Mater., 1 (3), 195-211.

62. Yakout, S. M., & Elsherif, E. (2010). Batch kinetics, isotherm and thermodynamic studies of adsorption of strontium from aqueous solutions onto low cost rice-straw based carbons, Carbon – Sci. Tech. 1, 144–153.

63. Yakubu, A., Olatunji, G. A., & Adekola, F. A. (2017). Synthesis and characterization of cellulose nanoparticles and its derivatives using a combination of spectro-analytical techniques. *Int J Nano Med & Eng*. 2(6), 65-94.

64. Zeng. L. (2004). Arsenic adsorption from aqueous solutions on a Fe (III)-Si binary oxide adsorbent. Water Qual. Res. J. Canada, 39 (3), 267-275.